

Fabrication of $\text{YBa}_2\text{Cu}_3\text{O}_7$ Superconducting Film on $\{100\}\langle 001 \rangle$ Textured Cu Tape via Conductive Buffer Layers*

Toshiya Doi^{1,3}, Masayuki Hashimoto¹, Shigeru Horii^{1,3} and Ataru Ichinose^{2,3}

¹Department of Energy Science and Technology, Graduate School of Energy Science, Kyoto University, Kyoto 606–8501, Japan

²Electric Power Engineering Research Laboratory, Central Research Institute of Electric Power Industry, Yokosuka 240–0196, Japan

³Japan Science and Technology Agency, ALCA, Tokyo 102–007, Japan

Long-length coated conductors (CCs) have recently become commercially available, serving as a promising candidate for use in electric power applications. However, the material and manufacturing costs are high, which discourages their use in a wide range of commercially feasible products.

$\text{REBa}_2\text{Cu}_3\text{O}_7$ (REBCO; RE: Y or rare-earth elements) superconducting films with high critical current density (J_c) have been grown on cube-textured metal tapes to develop CCs for high temperature, high magnetic field applications. In the standard approach, a biaxially oriented YBCO layer is deposited on a $\text{Y}_2\text{O}_3/\text{Y}_2\text{O}_3$ -stabilized $\text{ZrO}_2/\text{CeO}_2$ buffered Ni-W tape. CCs become highly resistive when they are quenched; therefore, for reliable and safe application, it is necessary to attach low-resistivity metal layers, such as Cu and/or Ag, to the CCs to stabilize and protect them from damage due to quenching. Presently, insulative oxides are used for the buffer layers; thus, thick Ag and Cu layers are required to be deposited as stabilizer layers on the YBCO layer. However, the high material and process costs for obtaining the Ag and Cu layers are one of the major obstacles to achieving low-cost CCs. The use of conductive buffer layers instead of insulative reduces the cost of CCs. In this paper, we propose a new configuration for CCs: YBCO deposited on a conductive $\text{Sr}(\text{Ti}_{0.95}\text{Nb}_{0.05})\text{O}_3$ buffered Ni-electroplated $\{100\}\langle 001 \rangle$ textured Cu and SUS316 lamination tape. $\text{Sr}(\text{Ti}_{0.95}\text{Nb}_{0.05})\text{O}_3$ was epitaxially grown on the Ni-electroplated $\{100\}\langle 001 \rangle$ textured Cu tape, and its resistivity was as low as 2.5 m Ω -cm at 77 K. An excellent J_c of 2.6×10^6 A/cm² was achieved at 77 K under a magnetic self-field for the YBCO/ $\text{Sr}(\text{Ti}_{0.95}\text{Nb}_{0.05})\text{O}_3$ /Ni/Cu/SUS316 tape. We believe that $\text{Sr}(\text{Ti}_{0.95}\text{Nb}_{0.05})\text{O}_3$ is a promising candidate for the conductive buffer layer material. [doi:10.2320/matertrans.M2017052]

(Received April 20, 2017; Accepted July 26, 2017; Published September 25, 2017)

Keywords: superconducting wire, critical current, $\text{YBa}_2\text{Cu}_3\text{O}_7$, cube texture, epitaxial growth, conductive buffer layer, critical current

1. Introduction

A superconducting material is an epoch-making material whose electrical resistance becomes zero by cooling. By using this ideal property of a conductor, a revolutionary product can be produced. In fact, numerous products such as medical MRI, nuclear magnetic resonance equipment, magnetic levitation trains, and accelerators cannot be realized without strong and uniform magnetic fields generated by electric wires (superconducting wire) fabricated using superconducting materials. The fact that the electrical resistance is zero means that there is absolutely no energy loss, and it is a breakthrough material from the viewpoint of efficient utilization of electrical energy. Nonetheless, the applications are limited to certain products. This is mainly because the superconducting wire must be cooled to cryogenic temperatures to achieve the superconducting state (currently, it is cooled using liquid helium with a boiling point of 4.2 K), and the equipment and operational cost is high. Therefore, considerable emphasis is placed on the practical application of a high-temperature superconducting material capable of realizing a superconducting state by cooling with liquid nitrogen (boiling point 77 K).

The irreversible magnetic field (effective critical magnetic field) of the high-temperature superconducting material depends strongly on its crystal structure^{1–5}; thus, the target material for developing the high-temperature superconducting wire is $\text{REBa}_2\text{Cu}_3\text{O}_7$ (REBCO; RE: Y or rare earth elements). $\text{YBa}_2\text{Cu}_3\text{O}_7$ (REBCOs are thought to be similar as

YBCO) has a relatively higher irreversible magnetic field at 77 K and has a high critical current density (J_c), even in strong magnetic fields; thus, it is expected to be applied used in various electric power applications. However, YBCO has the disadvantage that J_c decreases sharply when the grain boundary misorientation angle exceeds 10° ^{6,7}. Therefore, to obtain a YBCO superconducting wire with a practical J_c , we have to achieve biaxial crystal alignment (biaxial orientation) throughout the superconducting wire; this is an alignment in which the directions of the a-axis, b-axis, and c-axis of the YBCO crystal are all aligned as in a single crystal. When superconducting wire is used for various applications (e.g., magnets, MRI, and magnetic levitation trains), the length of the wire required is at least several hundred meters to one kilometer. Thus, to use the YBCO wire in practical applications, the YBCO crystals must be aligned biaxially in a length of several hundreds of meters.

To overcome this difficulty, new techniques have been developed to fabricate a biaxially oriented, high-temperature superconducting thin film on a metal tape using a thin film fabrication technique^{8–11}. Research and development are in progress in this regard. There are two methods to biaxially align the YBCO grains. The first is the IBAD method⁸, where a biaxially oriented oxide buffer layer is deposited on a Hastelloy tape by bombarding Ar ions during the buffer layer deposition from an oblique direction to form the template layer. The second is the RABiTS method^{9–11}, where rolling and recrystallized texture tapes are used for the template. There are numerous studies on high-temperature superconducting wires developed using both methods and both are currently commercially available from multiple wire manufacturers^{12–16}. Recently, the development of supercon-

*This Paper was Originally Published in Japanese in J. Japan Inst. Met. Mater. **80** (2016) 428–433.

ducting equipment using these commercially available high-temperature superconducting wires¹⁷⁾ has also been actively carried out. Moreover, it is considered that high-temperature superconducting wires have reached an almost practical level from a technical and performance point of view. However, as the price of the YBCO high-temperature superconducting wire is more than one order of magnitude higher than that of the Nb-Ti alloy superconducting wire currently used in MRI equipment and the like, it is not yet commercially viable.

Figure 1 shows a schematic of the IBAD^{12,13)} and RABiTS¹⁶⁾ wires. As both wires use a large amount of rare metals and precious metals (Ag), it is not likely that the wire price will decrease significantly, even during mass production. Furthermore, in the IBAD method, it is difficult to reduce the manufacturing cost dramatically because it is indispensable to form a film in vacuum using an ion beam (IBAD-MgO layer) to form a biaxially oriented layer. On the other hand, in the RABiTS method, the metal crystals of the substrate tape can be biaxially aligned by a simple method, combining cold rolling and heat treatment. There is a possibility that all processes can be carried out under atmospheric pressure in the future; thus, this method is more suitable for industrial production. In other words, if the YBCO wire is fabricated successfully on the textured metal tape without using rare metals and Ag, the price of the YBCO superconducting wires may reduce significantly.

We have developed a low-cost, high-temperature superconducting wire without using rare metals and Ag by epitaxially growing a conductive buffer layer and YBCO layers on a {100}<001> textured Cu tape obtained by cold rolling and recrystallization. Figure 2 shows a schematic of the proposed low-cost REBCO wire. In practical superconducting wires, a stabilizing layer is crucial for bypassing the current to recover the superconducting state when a disturbance has destroyed the superconducting state of some region. Usually, Cu is used for the stabilizing layer. For the commercially available IBAD and RABiTS wires, the electric resistances of the substrate metal tapes (Hastelloy or Ni-W) are high, and they cannot function as the stabilizing layer; thus, it is necessary to form an Ag layer and a Cu layer on the REBCO layer, which is a major obstacle for cost reduction. As shown in Fig. 2, using a pure Cu tape with a {100}<001> orientation as the substrate tape and using conductive oxides as the buffer layers, the Cu tape functions as not only the biaxially

oriented template, but also as the stabilizing layer. In other words, it may be possible to prepare a low-cost REBCO wire that does not require a large amount of expensive Ag or rare metals.

Thus far, we have reported that the biaxially oriented YBCO thin films with high J_c could be obtained on the {100}<001> textured Cu tapes¹⁸⁾. The YBCO thin film (270 nm thick) epitaxially grown on the Ni/CeO₂/YSZ (yttria stabilized zirconia)/CeO₂ buffered Cu/SUS316 lamination tape^{19–21)} had a high J_c of 3.6 MA/cm², and that it was possible to increase the film thickness while maintaining the J_c to obtain high J_c ^{22,23)}. The roles that the conductive buffer layers should satisfy are not only low electrical resistivity, but also structural compatibility and chemical inertness with Cu and REBCO, low diffusion coefficient of oxygen and metal elements. Thus, only a few attempts have so far been reported to develop conductive buffer layers on the Cu tape^{24,25)}. Aytug *et al.* reported that J_c of the YBCO thin film deposited on a Cu tape via conductive La_{0.7}Sr_{0.3}MnO₃/Ni double buffer layers was 2.3 MA/cm² at 77 K in self-field, and that insulative NiO layer, however, was formed at the La_{0.7}Sr_{0.3}MnO₃/Ni interface. Kim *et al.* reported that YBCO thin film grown on the (La, Sr)TiO₃/Ir buffered Cu tape has J_c of 1.0 MA/cm² at 77 K, and that Cu oxides, however, was observed on the surface of the YBCO film.

In this paper, we report the results for a new type of YBCO superconducting wire using Ni and Nb-doped SrTiO₃ as conductive buffer layers; this may realize a low-cost, high-temperature superconducting wire without using either expensive Ag or rare metal tapes (Hastelloy, Ni-W).

2. Experimental

Ni-electroplated Cu/SUS316 lamination tapes prepared by Tanaka Kikinzoku Kogyo KK (commercially available) were used as the substrates. An SUS316 tape with a thickness of 100 μm was bonded to a 30- μm -thick {100}<001> textured Cu tape, and a 0.5- μm -thick Ni layer was electro-deposited on the surface of the laminated tape (Ni/Cu/SUS tape)^{26,27)}. The crystal orientation of the Ni layer in the Ni/Cu/SUS tape was 5.0 to 5.5° (full width at half maximum (FWHM) value in the X-ray (111) ϕ -scan

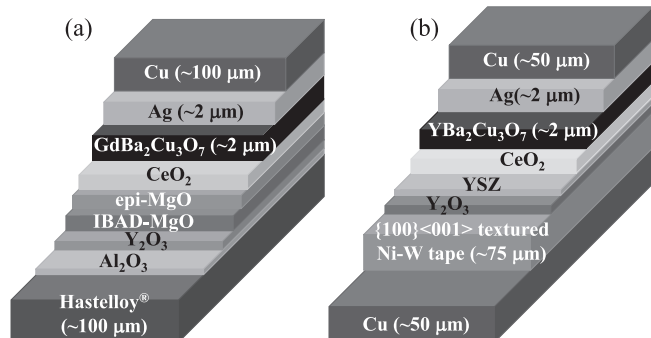


Fig. 1 Schematics of (a) IBAD and (b) RABiTS-type superconducting wires.

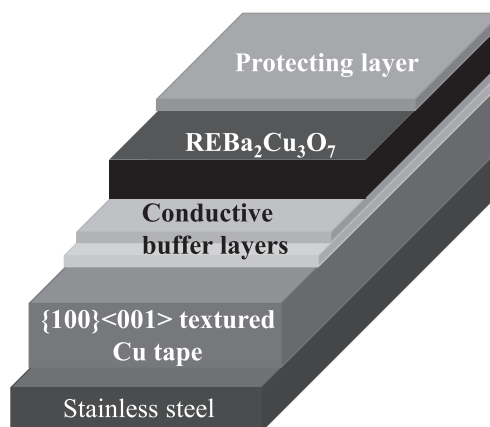


Fig. 2 Schematic of new superconducting wire with conductive buffer layers.

measurement).

Nb-doped SrTiO₃ (Nb-STO) was deposited in a 2% H₂ + 98% Ar atmosphere by a pulsed laser deposition (PLD) method using sintered bulk Sr(Ti_{0.95}Nb_{0.05})O_{3+δ} as the target. The pressure in the deposition chamber was 3.0×10^{-3} Pa, and the substrate temperature was changed from 600°C to 800°C. The 160-nm-thick YBCO layer was deposited by the PLD method in an oxygen atmosphere at 35 Pa and a substrate temperature of 790°C. After the deposition, annealing was performed under oxygen flow at 450°C for 16 h.

The crystal orientation of the prepared sample was evaluated by X-ray diffraction measurements (θ - 2θ method and pole figure method). The surface morphology of the sample was observed using scanning electron microscopy (SEM). The microstructure of the sample cross-section was observed using transmission electron microscopy (TEM, JEOL JEM-2100F). The TEM specimens were prepared by cutting and milling using a focused ion beam. Crystal orientation was also investigated by limited-field electron diffraction and nano-beam electron diffraction. Furthermore, elemental analysis by energy dispersive X-ray spectroscopy (EDX) was carried out to investigate the uniformity in the composition of the sample. The resistivity of the Nb-STO thin film and the critical current (I_c) of the YBCO thin film were measured by a standard 4-probe method. I_c was defined by an electric field criterion of $1 \mu\text{V}/\text{cm}$.

3. Results and Discussion

The Nb-STO thin films were prepared on the Ni/Cu/SUS tape at temperatures of 600, 700, and 800°C. Figure 3 shows the {110} pole figure of the samples prepared at 600 and 800°C. As strong X-ray diffraction intensities were observed at $(\psi, \phi) = (45^\circ, 0^\circ), (45^\circ, 90^\circ), (45^\circ, 180^\circ), (45^\circ, 270^\circ)$, it can be confirmed that the Nb-STO layers of both samples have a biaxial crystal orientation. The sample prepared at 700°C was also confirmed to be biaxially oriented (not shown in this figure). The FWHM obtained from the ϕ -scan measurements (intensity profile in ϕ direction) were $5.4^\circ, 6.0^\circ,$ and 6.2° for the samples fabricated at 600°C, 700°C, and 800°C, respectively. It was found that good biaxial orientation could be achieved for all samples and that the lower deposition temperature yielded a slightly better crystal orientation. We can see that Nb-STO is a very advantageous buffer layer material, considering the production of a long wire, because good biaxial orientation can be obtained in a very wide

deposition temperature range of 600°C to 800°C. The orientation relationship between Cu and Ni and the Nb-STO crystal was $(100)_{\text{Cu}}// (100)_{\text{Ni}}// (100)_{\text{Nb-STO}}$ and $[001]_{\text{Cu}}// [001]_{\text{Ni}}// [001]_{\text{Nb-STO}}$.

Figure 4 shows the SEM observation results for the surface of the Nb-STO thin films deposited on the Ni/Cu/SUS tapes with film thicknesses of 50, 100, 500, and 1000 nm. It was confirmed that when the film thickness was in the range of 50 to 500 nm, a good thin film with no cracks was obtained. However, for the 1000-nm-thick film, many cracks were observed parallel to the <110> direction on the film surface. It is found that the thickness of the Nb-STO layer had to be less than 1000 nm when using Nb-STO as a buffer layer on the Ni/Cu/SUS tape.

Next, to evaluate the resistivity, Nb-STO thin films were prepared on insulating MgO single crystal substrates under the same conditions as described above. Figure 5 (a) shows the deposition temperature dependence of the resistivity of the Nb-STO thin films measured at 300 K. The resistivity of the Nb-STO thin film prepared at 600°C exhibited a high value of $0.3 \Omega\cdot\text{cm}$. However, the resistivity at room temperature decreased rapidly with an increasing deposition temperature. The resistivity of the Nb-STO thin film prepared at 800°C was $6 \text{ m}\Omega\cdot\text{cm}$. Figure 5 (b) shows the temperature dependence of the resistivity of the film prepared at a substrate temperature of 800°C. In the range from room temperature to approximately 50 K, the resistivity decreased almost linearly as the sample temperature decreased, and the resistivity at 77 K was as low as $2.5 \text{ m}\Omega\cdot\text{cm}$.

Here, we consider whether this resistivity value is sufficiently low for a conductive buffer layer. The wire structure proposed in this study (Fig. 2) is based on the assumption that when a finite resistance is generated in the superconducting YBCO layer, the current flowing in the superconducting YBCO layer would be bypassed through the Nb-STO layer to the Cu tape. Assuming the tape width is 10 mm, the YBCO, Nb-STO, Ni, Cu, and SUS 316 layers have thicknesses of 2, 1, 0.5, 100, and 100 μm , respectively, and resistivities of $0.1 \times 10^{-3}, 2.5 \times 10^{-3}, 0.55 \times 10^{-6}, 0.2 \times 10^{-6},$ and $55 \times 10^{-6} \Omega\cdot\text{cm}$, respectively, where the electrical resistance of each layer at 77 K is calculated as follows. The resistances per centimeter in the longitudinal direction with respect to the current flowing in the longitudinal direction of the tape are calculated to be 0.5, 25, $1.1 \times 10^{-2}, 2 \times 10^{-5},$ and $5.5 \times 10^{-3} \Omega$ for the YBCO, Nb-STO, Ni, Cu, and SUS layer, respectively. When resistances are generated in the YBCO layer, almost all the current flows through the Cu layer in the longitudinal direction of the tape.

For the current flowing in the superconducting layer to flow into the Cu layer, the current must flow in the thickness direction from the YBCO layer to the Cu layer through the Nb-STO and Ni layers. The electrical resistances are calculated when the current passes through the Nb-STO and the Ni layers in the thickness direction. The electrical resistance of the Nb-STO layer with a thickness of $1 \mu\text{m}$ and an area of 1 cm^2 is $2.5 \times 10^{-7} \Omega$, and that of the Ni layer with a thickness of $0.5 \mu\text{m}$ and an area of 1 cm^2 is $2.8 \times 10^{-11} \Omega$. Thus, even when the thickness of the Nb-STO layer is set to be as thick as $1 \mu\text{m}$, the resistance of the current flowing in the film thickness direction is approximately 1/100 of the resis-

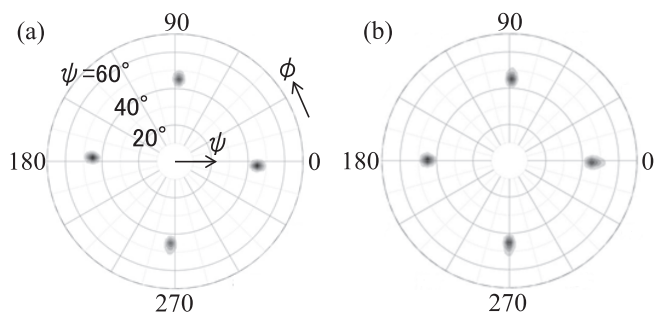


Fig. 3 X-ray {110} pole figures for the Nb-STO thin films prepared on the Ni/Cu/SUS tape at (a) 600 and (b) 800°C.

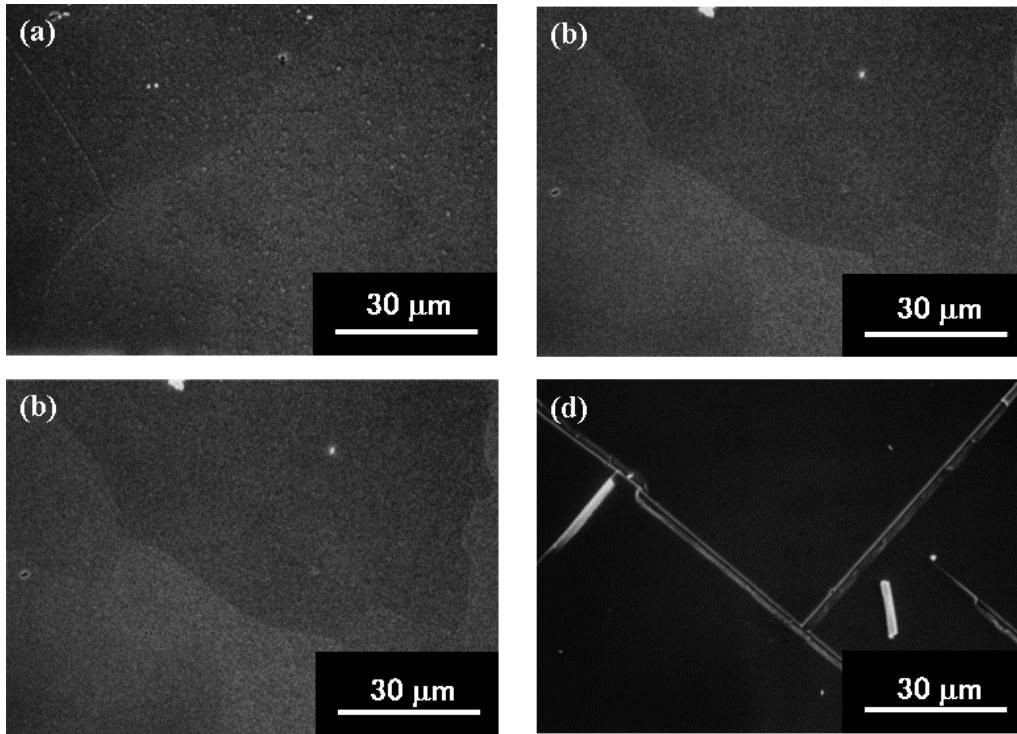


Fig. 4 SEM micrographs of the surfaces of the Nb-STO thin films prepared on the Ni/Cu/SUS tapes with thickness of (a) 50, (b) 100, (c) 500, and (d) 1000 nm.

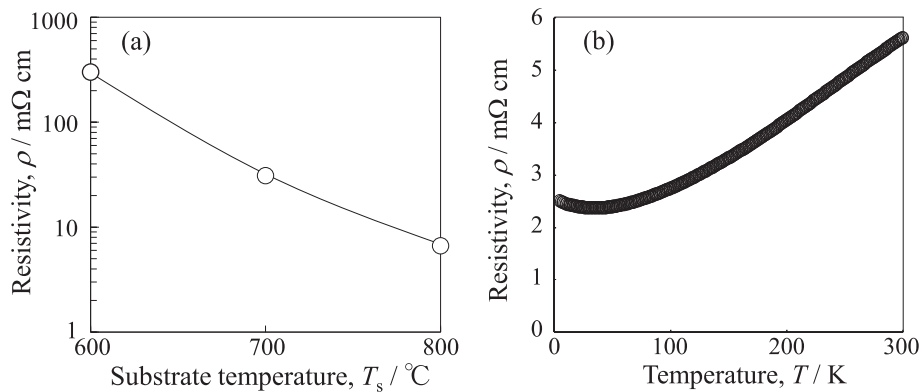


Fig. 5 (a) Substrate-temperature dependence of the resistivity of the Nb-STO thin films measured at 300 K and (b) temperature dependence of the resistivity of Nb-STO thin film prepared at 800°C. All specimens were prepared on MgO single crystal substrates.

tance when flowing in the longitudinal direction of the tape. The resistivity value of several mΩ for the Nb-STO layer seems to be sufficiently low for its use as a conductive buffer layer.

As described, we confirmed that the Nb-STO prepared on the Ni/Cu/SUS tape had sufficient biaxial orientation and low resistivity as the conductive buffer layer for the proposed YBCO superconducting wire. Then, we deposited the YBCO layer on the Nb-STO thin film.

Figures 6 (a) and 6 (b) show the X-ray θ - 2θ result and the (102) pole figure of YBCO for the sample with the 500-nm-thick YBCO thin film deposited on the 500-nm-thick Nb-STO layer prepared on the Ni/Cu/SUS tape. Only the (200) diffraction peaks of Cu, Ni, Nb-STO, and (00 l) diffraction peaks of the YBCO were observed in the X-ray θ - 2θ mea-

surement result, and in the (102) pole figure of YBCO, strong X-ray diffraction intensities were observed at only $(\psi, \phi) = (57^\circ, 0^\circ), (57^\circ, 90^\circ), (57^\circ, 180^\circ),$ and $(57^\circ, 270^\circ)$. These results show that the YBCO layer grown on the Nb-STO buffered Ni/Cu/SUS tape does not contain any secondary phases and has good biaxial crystal orientation.

Subsequently, the 160-nm-thick YBCO thin film was deposited on the 120-nm-thick Nb-STO layer prepared on the Ni/Cu/SUS tape (YBCO/Nb-STO/Ni/Cu/SUS). Figure 7 shows the current-voltage (I - V) characteristics of the YBCO/Nb-STO/Ni/Cu/SUS measured at 77 K in a magnetic self-field. The I_c of the sample was 13 A and J_c was calculated to be 2.6×10^6 A/cm², which was higher than those of commercially available RABiTS wires and at the same level as the IBAD wires.

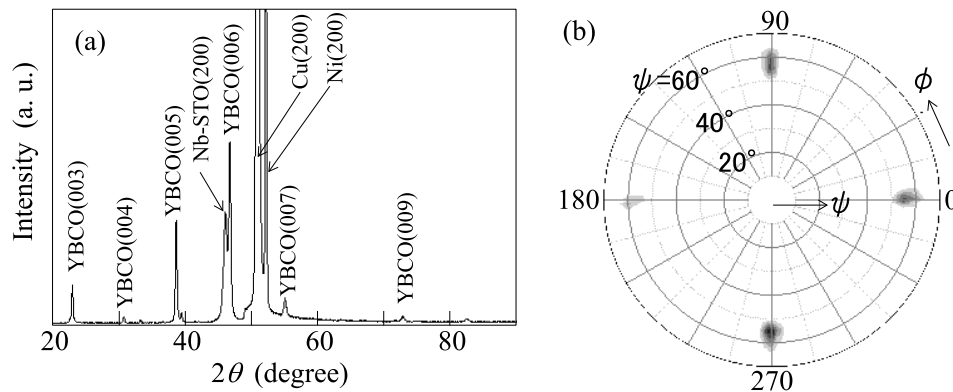


Fig. 6 (a) X-ray diffraction pattern and (b) X-ray $(102)_{\text{YBCO}}$ pole figure, obtained from the Nb-STO and YBCO deposited specimen on the Ni/Cu/SUS tape.

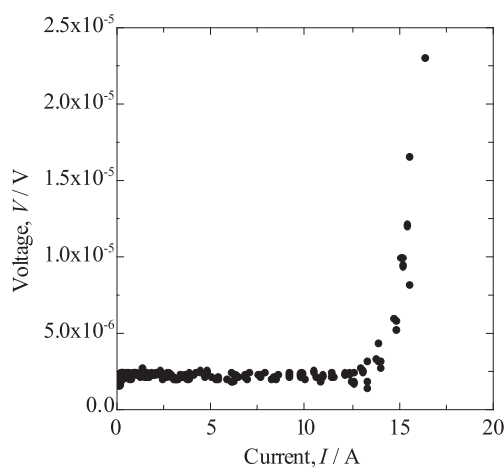


Fig. 7 I - V characteristics of the YBCO/Nb-STO/Ni/Cu/SUS tape measured at 77 K in magnetic self-field.

From these results, it is clear that it is possible to manufacture practical YBCO high-temperature superconducting wires with sufficiently high J_c , by using both $\{100\}\langle 001\rangle$ textured pure Cu tape and Ni and Nb-STO layers as the conductive buffer layers.

Figures 8 (a) and 8 (b) show bright field images (BFI) for the cross-sections of the samples after the I_c measurement by scanning transmission electron microscopy (STEM) at low magnification and high magnification, respectively. From Fig. 8 (a), it can be seen that a good YBCO layer was obtained over a wide region. In addition, although the grain boundary of Cu is present at the left end of the figure, the Nb-STO layer and the YBCO layer on the upper part of the figure are not subject to the grain boundary of the Cu and their crystal growth occurs smoothly in the direction parallel to the tape. When fabricating REBCO wires using the RABiTS method, there is a concern that the J_c may decrease owing to the existence of a groove at the grain boundaries on the surface of the metal tape, such as Ni-W or Cu. However, we confirmed that the groove problem does not occur in the case of the Cu tape.

As the interface between the Cu tape and the Ni layer was unclear, it can be seen that some interdiffusion occurs between them. The interface between the YBCO and the Nb-

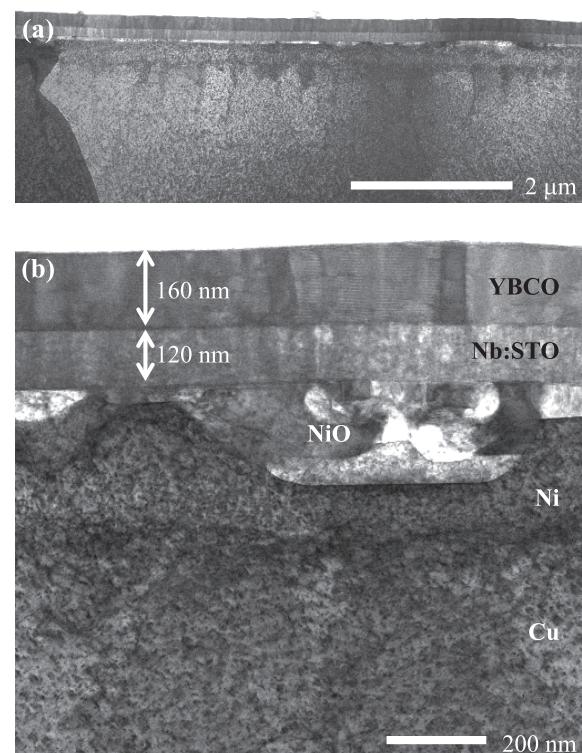


Fig. 8 Cross-sectional STEM images of the YBCO/Nb-STO/Ni/Cu/SUS tape at (a) low and (b) high magnifications.

STO layers was clean and sharp. A white layer of several tens of nm thick was observed at the interface between the Nb-STO and the Ni layers. Figure 8 (b) shows a magnified image observed near a region where this white layer became relatively thick. From the EDX analysis (described later), we confirmed that this white layer was NiO. Since the interface between the Nb-STO and the NiO layers is flat, the NiO layer was not formed at the time of film formation of the Nb-STO layer. Oxygen atoms from the YBCO layer arrived at the Ni layer through the Nb-STO layer during the YBCO deposition, and the NiO layer was generated by oxidizing the Ni layer from the Nb-STO layer side.

Figure 9 shows the EDX elemental mapping images of Sr, O, Ni, Y, and Cu for the region corresponding to the STEM image of the sample. The mapping results of O and Ni indi-

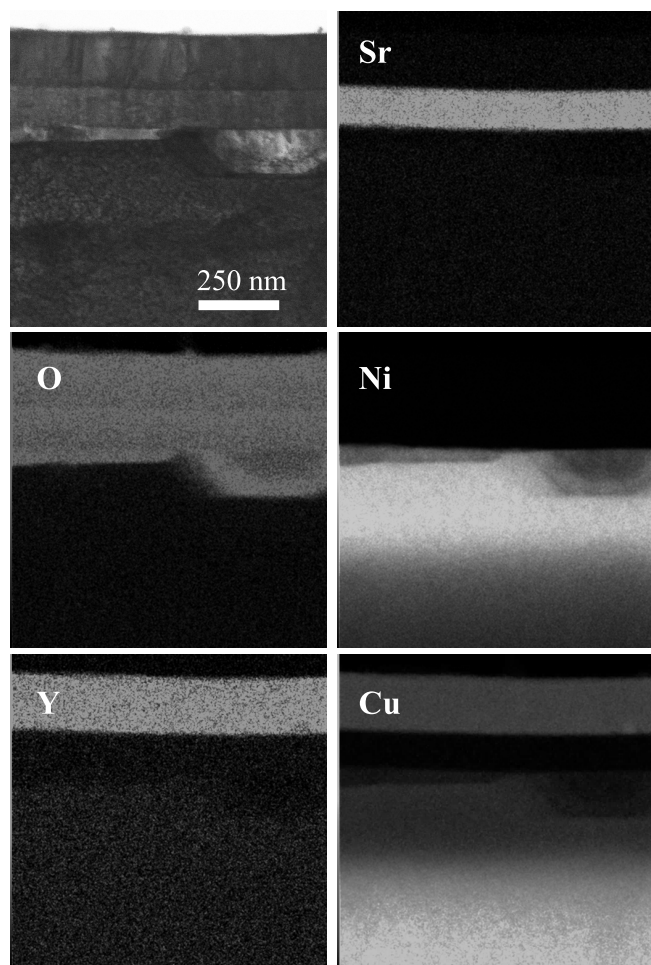


Fig. 9 STEM images of the YBCO/Nb-STO/Ni/Cu/SUS tape and EDX mapping images of Sr, O, Ni, Y, and Cu elements in the same region.

cate that the white layer formed directly under the Nb-STO layer in Fig. 8 was NiO. In addition, from the mapping results of Ni and Cu, it can be confirmed that the diffusions of Ni and Cu were blocked by the Nb-STO layer, and neither Ni nor Cu entered the YBCO layer. It can also be confirmed that there was no interdiffusion between the Nb-STO layer and the YBCO layer.

We confirmed that Nb-STO could block the diffusion of Ni even if it is a relatively thin layer of 120 nm, and that it can block the interdiffusion of metal elements between the Ni/Cu/SUS tape and the YBCO layer. However, since oxygen is slightly diffused, the formation of a thin NiO layer of several tens of nm could not be avoided at the interface between the Ni and the Nb-STO layers. Since NiO is insulative at low temperatures, the existence of the NiO at the interface hinders the current flowing in the YBCO superconducting layer from bypassing to the Cu tape when the superconducting state of the YBCO layer breaks down. However, in this study, the thickness of the Nb-STO layer was set to 120 nm for the I_c measurement specimen. The thickness of the Nb-STO layer can increase easily to 500 nm without any crack formation. By increasing the thickness of the Nb-STO layer to approximately 500 nm, oxygen diffusion through the Nb-STO layer during the YBCO deposition was reduced drastically and the formation of NiO layer could be avoided.

Alternatively, as we confirmed that Nb-STO is a conductive buffer layer blocking the diffusion of Ni, we developed a new conductive buffer layer with a small oxygen diffusion coefficient. Then, by combining the new conductive buffer layer and Nb-STO/Ni/Cu/SUS structure, the formation of a NiO layer is thought to be avoided.

4. Conclusion

We propose a novel $\text{REBa}_2\text{Cu}_3\text{O}_7$ high-temperature superconducting wire that can be fabricated without using a large amount of rare metals, such as Ni, W, and Co, and precious metals, such as Ag. The material cost can be reduced drastically by using the conductive buffer layers and the pure Cu tape simultaneously placing the rolls of the template and stabilizer layer on Cu, which is essential for a practical superconducting wire. To realize the proposed new high-temperature superconducting wire, the buffer layer must be prepared using conductive materials. In this study, we used pure Cu tape with a $\{100\}\langle 001 \rangle$ texture as the biaxially oriented template layer and electrical stabilizing layer. The Cu tape was laminated with SUS316 tape to enhance the mechanical strength of the wire, and Ni and $\text{Sr}(\text{Ti}_{0.95}\text{Nb}_{0.05})\text{O}_3$ were used as the conductive buffer layers. We confirmed that the $\text{Sr}(\text{Ti}_{0.95}\text{Nb}_{0.05})\text{O}_3$ layer deposited on the Ni/Cu/SUS tape showed excellent biaxial crystal orientation and worked as an effective diffusion-block-layer for Ni and Cu. We showed that the $\text{Sr}(\text{Ti}_{0.95}\text{Nb}_{0.05})\text{O}_3$ is one of the promising conductive buffer layer materials suitable for obtaining a high J_c YBCO layer. However, slight oxygen diffusion occurs through $\text{Sr}(\text{Ti}_{0.95}\text{Nb}_{0.05})\text{O}_3$ from the YBCO layer to the Ni layer; the $\text{Sr}(\text{Ti}_{0.95}\text{Nb}_{0.05})\text{O}_3$ buffer allows the formation of an undesirable NiO layer. Henceforth, to realize the proposed low-cost REBCO high-temperature superconducting wire with a novel structure, some measures to prevent oxygen diffusion are necessary.

REFERENCES

- 1) J.R. Clem: *Phys. Rev. B* **43** (1991) 7837–7846.
- 2) D.H. Kim, K.E. Gray, R.T. Kampwirth, J.C. Smith, D.S. Richeson, T.J. Marks and M. Eddy: *Physica C* **177** (1991) 431–437.
- 3) T. Doi, M. Okada, A. Soeta, T. Yuasa, K. Aihara, T. Kamo and S. Matsuda: *Physica C* **183** (1991) 67–72.
- 4) T. Nabatame, Y. Saito, T. Doi, T. Kamo and S. Matsuda: *Physica C* **190** (1991) 114–115.
- 5) J. Shimoyama and K. Kishio: *OYO BUTURI* **73** (2004) 14–21.
- 6) D. Dimos, P. Chaudhari, J. Manhart and F.K. Legoues: *Phys. Rev. Lett.* **61** (1988) 219–222.
- 7) D. Dimos, P. Chaudhari and J. Manhart: *Phys. Rev. B* **41** (1990) 4038–4049.
- 8) Y. Iijima, N. Tanabe, O. Kohno and Y. Ikeno: *Appl. Phys. Lett.* **60** (1992) 769–771.
- 9) T. J. Doi, T. Yuasa, T. Ozawa and K. Higashiyama: *Advances in Superconductivity VII*, Eds. K. Yamafuji & T. Morishita, (Springer-Verlag, Tokyo, 1995) 817–820.
- 10) T. Doi and K. Higashiyama: *OYO BUTURI* **65** (1996) 372–376.
- 11) A. Goyal, D.P. Norton, J.D. Budai, M. Paranthaman, E.D. Specht, D.M. Kroeger, D.K. Christen, Q. He, B. Saffian, F.A. List, D.F. Lee, P.M. Martin, C.E. Klabunde, E. Hartfield and V.K. Sikka: *Appl. Phys. Lett.* **69** (1996) 1795–1797.
- 12) <http://www.fujikura.co.jp/products/new/superconductor/nd1001.html>
- 13) <http://www.superpower-inc.com/>

- 14) <http://www.i-sunam.com/>
- 15) <http://www.superox.ru/en/products/42-2G-HTS-tape/>
- 16) http://www.amsc.com/solutions-products/hts_wire.html
- 17) Y. Shiohara: *J. IEE Japan* **134** (2014) 540–541.
- 18) M. Tokudome, T. Doi, R. Tomiyasu, S. Sato, Y. Hakuraku, S. Kubota, K. Shima, N. Kashima and S. Nagaya: *J. Appl. Phys.* **104** (2008) 103913.
- 19) M. Tokudome, T. Doi, R. Tomiyasu, M. Daio, Y. Hakuraku, K. Shima, S. Kubota, N. Kashima and S. Nagaya: *IEEE Trans. Appl. Supercond.* **19** (2009) 3287–3290.
- 20) R. Tomiyasu, T. Doi, M. Tokudome, M. Daio, Y. Hakuraku, S. Kubota, K. Shima, N. Kashima and S. Nagaya: *TEION KOGAKU* **43** (2008) 269–277.
- 21) M. Daio, T. Doi, Y. Hakuraku, S. Kubota, K. Shima, N. Kashima and S. Nagaya: *TEION KOGAKU* **44** (2009) 488–495.
- 22) I. Gi, T. Doi, A. Katsume, T. Miyana, M. Inada, Y. Hakuraku, S. Kubota, K. Shima, N. Kashima and S. Nagaya: *TEION KOGAKU* **47** (2012) 276–281.
- 23) T. Miyana, T. Doi, M. Inada, H. Ohara, D. Hirata, Y. Hakuraku, K. Shima, S. Kubota, N. Kashima and S. Nagaya: *TEION KOGAKU* **47** (2012) 667–673.
- 24) T. Aytug, M. Paranthaman, J.R. Thompson, A. Goyal, N. Rutter, H.Y. Zhai, A.A. Gapud, A.O. Ijaluola and D.K. Christen: *Appl. Phys. Lett.* **83** (2003) 3963–3965.
- 25) K. Kim, D.P. Norton, C. Cantoni, T. Aytug, A.A. Gapud, M.P. Paranthaman, A. Goyal and D.K. Christen: *IEEE Trans. Appl. Supercond.* **15** (2005) 2997–3000.
- 26) N. Kashima, K. Shima, T. Doi, S. Kubota, T. Watanabe, M. Inoue, T. Kiss and S. Nagaya: *IEEE Trans. Appl. Supercond.* **19** (2009) 3299–3302.
- 27) N. Kashima, S. Kubota, K. Shima, T. Doi, S. Nagaya, M. Inoue and T. Kiss: *Jpn. J. Appl. Phys.* **50** (2011) 063101.